Supporting Material

A modular view of the diversity of cell-density-encoding schemes in bacterial quorum-sensing systems

Bastian Drees, Matthias Reiger, Kirsten Jung* and Ilka B. Bischofs*
Zentrum für Molekulare Biologie and BioQuant,
University of Heidelberg, Germany

* To whom correspondence should be addressed:

e-mail: i.bischofs@zmbh.uni-heidelberg.de

e-mail: Kirsten.Jung@lrz.uni-muenchen.de

Supporting Figure S1:

Classification of basic encoder architectures: (A) Encoder architectures can be classified based on network topology: Signal modification determines the general topology of the network and thereby the complexity of the system. (B) Cross classification matrix reporting the number of architectures in each category spanned by network topology and encoder function. Almost all classes can be built from almost all network structures. Total numbers of systems in each encoder class or network topology class are shown on the sides. (C) Network feature analysis: Occurrence of different architectural features in the four basic encoder classes. 3rd panel: Intracellular modification can be integrated with production π into one single production step of molecules *B**. Thus molecules *A* and *B** can be viewed as *unmodified**.

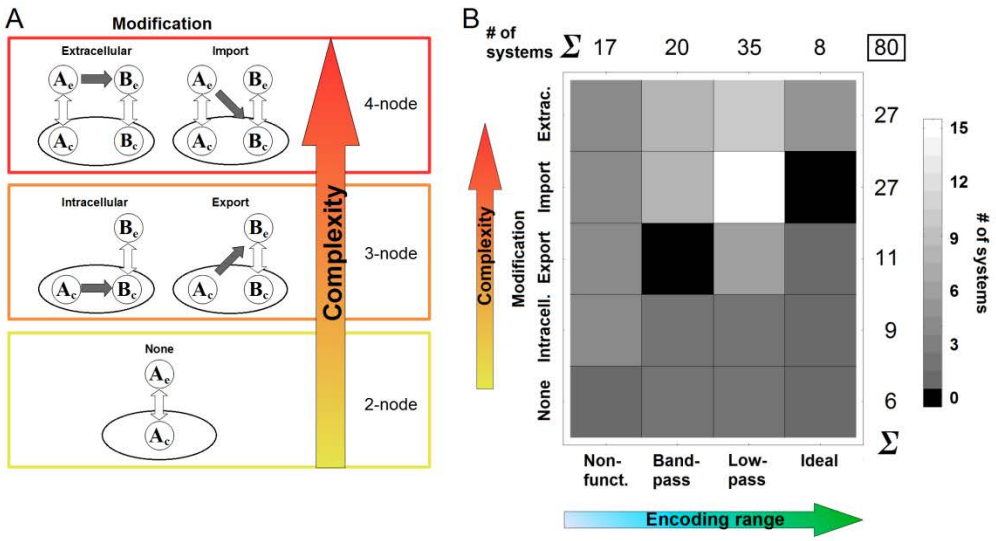

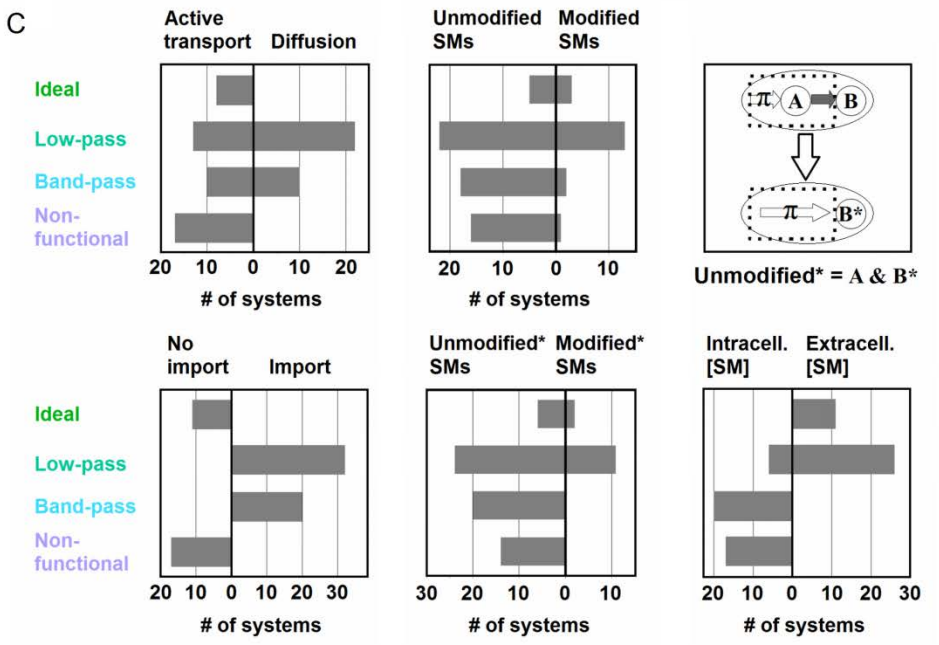

Supporting Figure S2:

Approximation of Noise decomposition: Exact results (solid, blue line) and approximate decomposition (dashed, red line) of noise characteristics of 4-node networks.

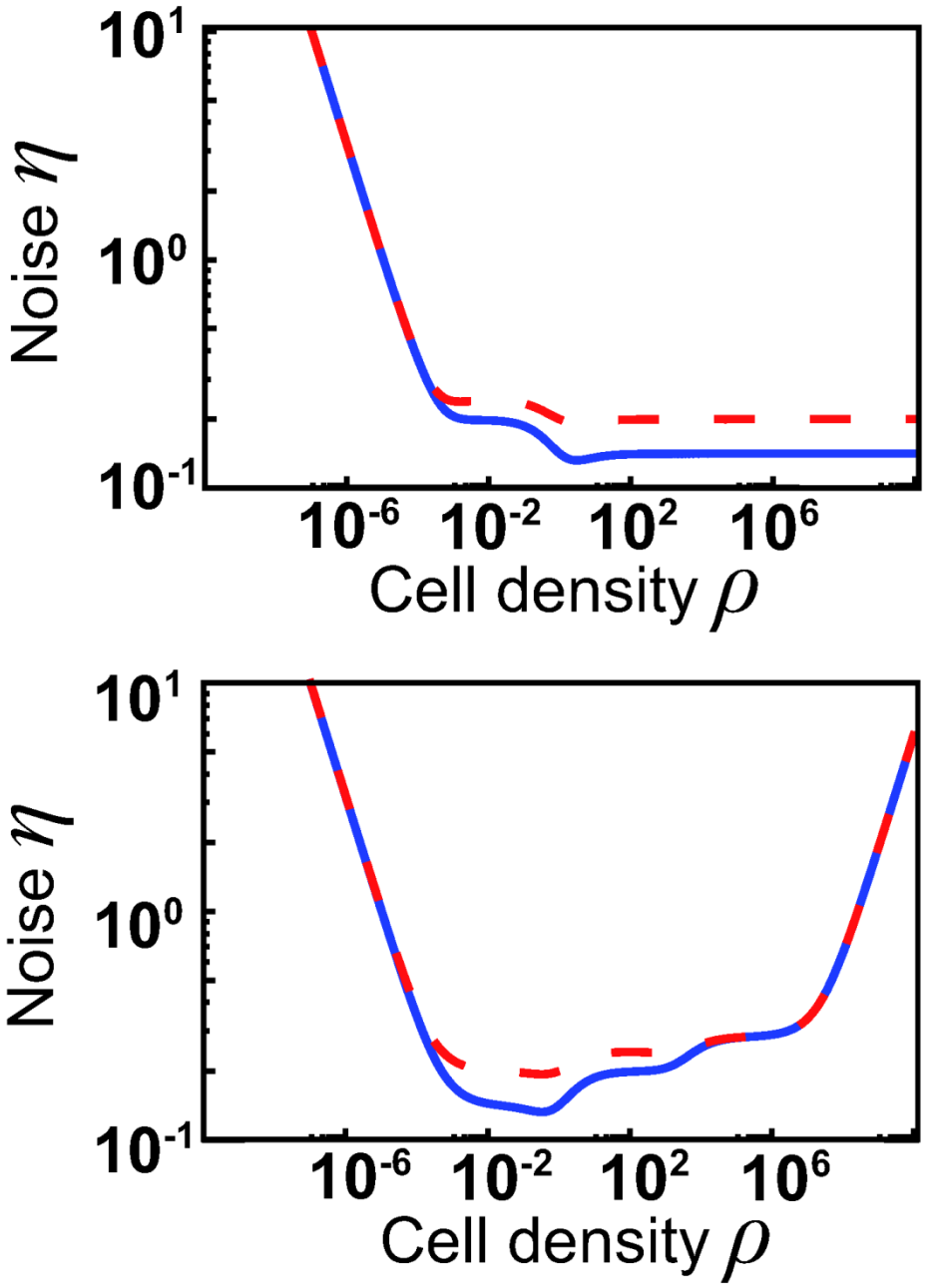

Supporting Figure S3:

Influence of feedback on the three functional basic classes: Feedback leaves the encoding behavior unchanged at high and low cell densities, but increases the sensitivity in the input range, where it sets in. We investigated the influence of feedback on the production by substituting the constant production rate by a term $\pi_o + \pi_{fb}\frac{[SM]}{[SM]+K}$, where π_o is the un-induced basal production rate, π_{fb} the up-regulated production rate and K the value of the SM concentration at which the feedback is half maximal. Supporting figure S2 shows the results for the three basic encoder classes, band-pass, low-pass and ideal. While the encoding behavior remains the same for high and low cell densities, the sensitivity is increased in all three cases in the input range, where the SM concentration is in the same order of magnitude as K. For the plots in supporting figure S2 we used $\pi_o = 100\frac{\text{nM}}{\text{h}}$, $\pi_{fb} = 10000\frac{\text{nM}}{\text{h}}$ and $K = 1000\text{nM}$.

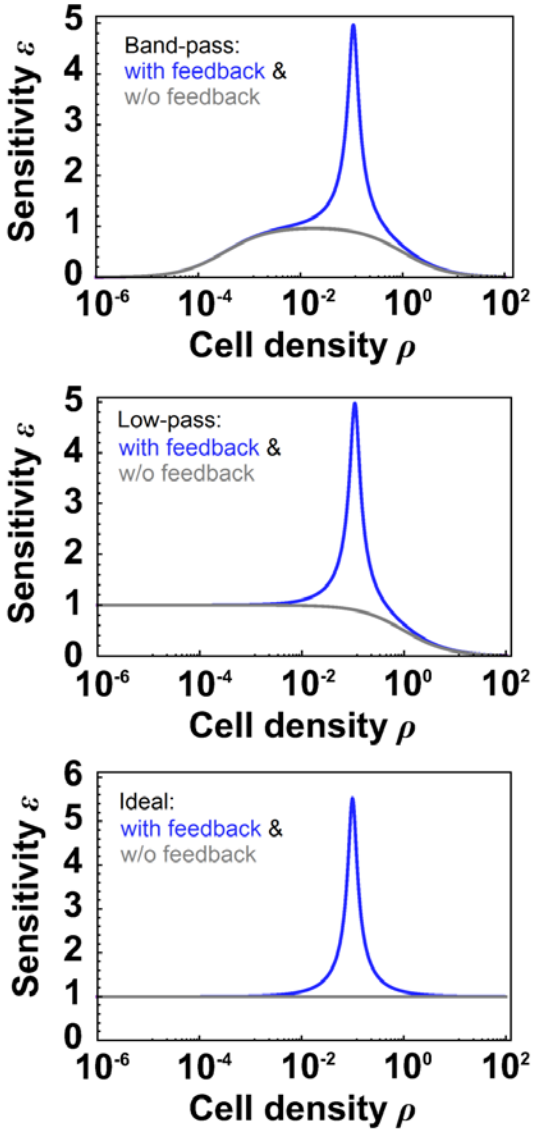

Table S1 - Strains used in this study.

Strain	Relevant genotype or description	Reference or source
Vibrio harveyi BB120	Wild type, ATCC BAA-1116	(1)
Vibrio harveyi MR3	Δ*luxS* (AI-2$^-$)	This work
E. coli DH5α λ*pir*	*Δ(argF-lac)169* φ80d*lacZ58*(M15) *glnV44*(AS) *relA1 gyrA96*(NalR), *recA1 endA1 thiE1 hsdR17 λpir*	(2)
E. coli WM3064	*thrB1*004 *pro thi rpsL hsdS lacZ*ΔM15 RP4-1360 Δ(*araBAD*)567 Δ*dapA*1341::[*erm pir*(wt)]	W. Metcalf, Univ. of Illinois, Urbana

Table S2 - Plasmids used in this study.

Plasmid	Relevant genotype or description	Reference or source
pNPTS138-R6KT	*mobRP4*$^+$ *ori-R6K sacB*; suicide plasmid for in-frame deletions; Kan^r	(3)
pNPTS138-R6KT-Δ*luxS*	*luxS* deletion fragment in pNPTS138-R6KT	This work
pBBR1-MCS-2-*lacZ*	broad-host-range cloning vector with reporter *lacZ*; Kan^r	(4)
pBBR1-MCS2-*lsrKR*P$_{lsr}$::*lacZ*	*lsrKR*P$_{lsr}$ cloned into the *Eco*RI and *Nco*I sites of pBBR1-MCS-2-*lacZ*	This work

Table S3 - Classification of architectures

Column *Struct.* denotes whether there is no modification (NM) or intracellular modification (IC), modification during export (ExpM), during import (ImpM) or extracellular (ECM). The column *Parameter changes* refers to the parameter changes that have been done compared to the generic structure shown in the equations in Supplementary Methods S1. Column *[SM]* denotes the SM concentration measured by the respective system and column *Class* the class the system belongs to: i.e. non-functional (NF), band-pass (BP), low-pass (LP), ideal (ID), band-pass ultrasensitive (BPU), multi-pass (MP), low-pass ultrasensitive (LPU), ideal ultrasensitive (IDU), negative sensitivity (NS). Highlighted systems have been used for the plots in Fig.3 and 4 in the main text.

Struct.	**Parameter changes**	**[SM]**	**Class**	**Struct.**	**Parameter changes**	**[SM]**	**Class**
NM	none	A_c	BP	ImpM	$\theta_{in,A}, \theta_{out,A} \rightarrow \theta_{diff,A}$	B_e	LPU
NM	none	A_e	LP	ImpM	$\theta_{in,B} = 0$	B_c	LP
NM	$\theta_{in,A} = 0$	A_c	NF	ImpM	$\theta_{in,B} = 0$	B_e	IDU
NM	$\theta_{in,A} = 0$	A_e	ID	ImpM	$\theta_{in,B}, \theta_{out,B} \rightarrow \theta_{diff,B}$	B_c	BPU/MP
NM	$\theta_{in,A}, \theta_{out,A} \rightarrow \theta_{diff,A}$	A_c	BP	ImpM	$\theta_{in,B}, \theta_{out,B} \rightarrow \theta_{diff,B}$	B_e	LPU
NM	$\theta_{in,A}, \theta_{out,A} \rightarrow \theta_{diff,A}$	A_e	LP	ImpM	$\theta_{in,A} = 0; \theta_{in,B} = 0$	B_c	LP
ICM	none	A_c	NF	ImpM	$\theta_{in,A} = 0; \theta_{in,B} = 0$	B_e	IDU
ICM	none	B_c	BP	ImpM	$\theta_{in,A} = 0; \theta_{in,B}, \theta_{out,B} \rightarrow \theta_{diff,B}$	B_c	BPU/MP
ICM	none	B_e	LP	ImpM	$\theta_{in,A} = 0; \theta_{in,B}, \theta_{out,B} \rightarrow \theta_{diff,B}$	B_e	LPU
ICM	$\theta_{in} = 0$	A_c	NF	ImpM	$\theta_{in,A}, \theta_{out,A} \rightarrow \theta_{diff,A}; \theta_{in,B} = 0$	B_c	LP
ICM	$\theta_{in} = 0$	B_c	NF	ImpM	$\theta_{in,A}, \theta_{out,A} \rightarrow \theta_{diff,A}; \theta_{in,B} = 0$	B_e	IDU
ICM	$\theta_{in} = 0$	B_e	ID	ImpM	$\theta_{in,A}, \theta_{out,A} \rightarrow \theta_{diff,A}$; $\theta_{in,B}, \theta_{out,B} \rightarrow \theta_{diff,B}$	B_c	BPU/MP
ICM	$\theta_{in}, \theta_{out} \rightarrow \theta_{diff}$	A_c	NF	ImpM	$\theta_{in,A}, \theta_{out,A} \rightarrow \theta_{diff,A}$; $\theta_{in,B}, \theta_{out,B} \rightarrow \theta_{diff,B}$	B_e	LPU
ICM	$\theta_{in}, \theta_{out} \rightarrow \theta_{diff}$	B_c	BP	ECM	None	A_c	BP
ICM	$\theta_{in}, \theta_{out} \rightarrow \theta_{diff}$	B_e	LP	ECM	None	A_e	LP
ExpM	none	A_c	NF	ECM	$\theta_{in,A} = 0$	A_c	NF
ExpM	none	B_c	LP	ECM	$\theta_{in,A} = 0$	A_e	ID
ExpM	none	B_e	LP	ECM	$\theta_{in,A}, \theta_{out,A} \rightarrow \theta_{diff,A}$	A_c	BP
ExpM	$\theta_{out} = 0$	A_c	NF	ECM	$\theta_{in,A}, \theta_{out,A} \rightarrow \theta_{diff,A}$	A_e	LP
ExpM	$\theta_{out} = 0$	B_c	LP	ECM	$\theta_{out,B} = 0$	A_c	BP
ExpM	$\theta_{out} = 0$	B_e	LP	ECM	$\theta_{out,B} = 0$	A_e	LP
ExpM	$\theta_{in}, \theta_{out} \rightarrow \theta_{diff}$	A_c	NF	ECM	$\theta_{in,B}, \theta_{out,B} \rightarrow \theta_{diff,B}$	A_c	BP
ExpM	$\theta_{in}, \theta_{out} \rightarrow \theta_{diff}$	B_c	LP	ECM	$\theta_{in,B}, \theta_{out,B} \rightarrow \theta_{diff,B}$	A_e	LP
ExpM	$\theta_{in}, \theta_{out} \rightarrow \theta_{diff}$	B_e	LP	ECM	$\theta_{in,A} = 0; \theta_{out,B} = 0$	A_c	NF
ExpM	$\theta_{in} = 0$	A_c	NF	ECM	$\theta_{in,A} = 0; \theta_{out,B} = 0$	A_e	ID
ExpM	$\theta_{in} = 0$	B_e	ID	ECM	$\theta_{in,A} = 0; \theta_{in,B}, \theta_{out,B} \rightarrow \theta_{diff,B}$	A_c	NF

ImpM	none	A_c	BP		ECM	$\theta_{in,A} = 0$; $\theta_{in,B}$, $\theta_{out,B} \rightarrow \theta_{diff,B}$	A_e	ID
ImpM	none	A_e	LP		ECM	$\theta_{in,A}$, $\theta_{out,A} \rightarrow \theta_{diff,A}$; $\theta_{in,B} = 0$	A_c	BP
ImpM	$\theta_{in,A} = 0$	A_c	NF		ECM	$\theta_{in,A}$, $\theta_{out,A} \rightarrow \theta_{diff,A}$; $\theta_{in,B} = 0$	A_e	LP
ImpM	$\theta_{in,A} = 0$	A_e	LP		ECM	$\theta_{in,A}$, $\theta_{out,A} \rightarrow \theta_{diff,A}$; $\theta_{in,B}$, $\theta_{out,B} \rightarrow \theta_{diff,B}$	A_c	BP
ImpM	$\theta_{in,A}$, $\theta_{out,A} \rightarrow \theta_{diff,A}$	A_c	BP		ECM	$\theta_{in,A}$, $\theta_{out,A} \rightarrow \theta_{diff,A}$; $\theta_{in,B}$, $\theta_{out,B} \rightarrow \theta_{diff,B}$	A_e	LP
ImpM	$\theta_{in,A}$, $\theta_{out,A} \rightarrow \theta_{diff,A}$	A_e	LP		ECM	$\theta_{in,B} = 0$	A_c	BP
ImpM	$\theta_{in,B} = 0$	A_c	BP		ECM	$\theta_{in,B} = 0$	A_e	LP
ImpM	$\theta_{in,B} = 0$	A_e	LP		ECM	$\theta_{in,B} = 0$	B_e	LP
ImpM	$\theta_{in,B}$, $\theta_{out,B} \rightarrow \theta_{diff,B}$	A_c	BP		ECM	$\theta_{in,A} = 0$; $\theta_{in,B} = 0$	A_c	NF
ImpM	$\theta_{in,B}$, $\theta_{out,B} \rightarrow \theta_{diff,B}$	A_e	LP		ECM	$\theta_{in,A} = 0$; $\theta_{in,B} = 0$	A_e	ID
ImpM	$\theta_{in,A} = 0$; $\theta_{in,B} = 0$	A_c	NF		ECM	$\theta_{in,A} = 0$; $\theta_{in,B} = 0$	B_e	ID
ImpM	$\theta_{in,A} = 0$; $\theta_{in,B} = 0$	A_e	LP		ECM	$\theta_{in,A}$, $\theta_{out,A} \rightarrow \theta_{diff,A}$; $\theta_{in,B} = 0$	A_c	BP
ImpM	$\theta_{in,A} = 0$; $\theta_{in,B}$, $\theta_{out,B} \rightarrow \theta_{diff,B}$	A_c	NF		ECM	$\theta_{in,A}$, $\theta_{out,A} \rightarrow \theta_{diff,A}$; $\theta_{in,B} = 0$	A_e	LP
ImpM	$\theta_{in,A} = 0$; $\theta_{in,B}$, $\theta_{out,B} \rightarrow \theta_{diff,B}$	A_e	LP		ECM	$\theta_{in,A}$, $\theta_{out,A} \rightarrow \theta_{diff,A}$; $\theta_{in,B} = 0$	B_e	LP
ImpM	$\theta_{in,A}$, $\theta_{out,A} \rightarrow \theta_{diff,A}$; $\theta_{in,B} = 0$	A_c	BP		ECM	None	B_c	NS
ImpM	$\theta_{in,A}$, $\theta_{out,A} \rightarrow \theta_{diff,A}$; $\theta_{in,B} = 0$	A_e	LP		ECM	None	B_e	NS
ImpM	$\theta_{in,A}$, $\theta_{out,A} \rightarrow \theta_{diff,A}$; $\theta_{in,B}$, $\theta_{out,B} \rightarrow \theta_{diff,B}$	A_c	BP		ECM	$\theta_{in,A} = 0$	B_c	LP
ImpM	$\theta_{in,A}$, $\theta_{out,A} \rightarrow \theta_{diff,A}$; $\theta_{in,B}$, $\theta_{out,B} \rightarrow \theta_{diff,B}$	A_e	LP		ECM	$\theta_{in,A} = 0$	B_e	LP
ImpM	$\theta_{out,B} = 0$	A_c	BP		ECM	$\theta_{in,A}$, $\theta_{out,A} \rightarrow \theta_{diff,A}$	B_c	NS
ImpM	$\theta_{out,B} = 0$	A_e	LP		ECM	$\theta_{in,A}$, $\theta_{out,A} \rightarrow \theta_{diff,A}$	B_e	NS
ImpM	$\theta_{out,B} = 0$	B_c	LP		ECM	$\theta_{out,B} = 0$	B_c	NS
ImpM	$\theta_{in,A} = 0$; $\theta_{out,B} = 0$	A_c	NF		ECM	$\theta_{out,B} = 0$	B_e	NS
ImpM	$\theta_{in,A} = 0$; $\theta_{out,B} = 0$	A_e	LP		ECM	$\theta_{in,B}$, $\theta_{out,B} \rightarrow \theta_{diff,B}$	B_c	NS
ImpM	$\theta_{in,A} = 0$; $\theta_{out,B} = 0$	B_c	LP		ECM	$\theta_{in,B}$, $\theta_{out,B} \rightarrow \theta_{diff,B}$	B_e	NS
ImpM	$\theta_{in,A}$, $\theta_{out,A} \rightarrow \theta_{diff,A}$; $\theta_{out,B} = 0$	A_c	BP		ECM	$\theta_{in,A} = 0$; $\theta_{out,B} = 0$	B_c	LP
ImpM	$\theta_{in,A}$, $\theta_{out,A} \rightarrow \theta_{diff,A}$; $\theta_{out,B} = 0$	A_e	LP		ECM	$\theta_{in,A} = 0$; $\theta_{out,B} = 0$	B_e	LP
ImpM	$\theta_{in,A}$, $\theta_{out,A} \rightarrow \theta_{diff,A}$; $\theta_{out,B} = 0$	B_c	LP		ECM	$\theta_{in,A} = 0$; $\theta_{in,B}$, $\theta_{out,B} \rightarrow \theta_{diff,B}$	B_c	LP
ImpM	none	B_c	BPU/MP		ECM	$\theta_{in,A} = 0$; $\theta_{in,B}$, $\theta_{out,B} \rightarrow \theta_{diff,B}$	B_e	LP
ImpM	none	B_e	LPU		ECM	$\theta_{in,A}$, $\theta_{out,A} \rightarrow \theta_{diff,A}$; $\theta_{in,B}$, $\theta_{out,B} \rightarrow \theta_{diff,B}$	B_c	NS
ImpM	$\theta_{in,A} = 0$	B_c	BPU/MP		ECM	$\theta_{in,A}$, $\theta_{out,A} \rightarrow \theta_{diff,A}$; $\theta_{in,B}$, $\theta_{out,B} \rightarrow \theta_{diff,B}$	B_e	NS
ImpM	$\theta_{in,A} = 0$	B_e	LPU		ECM	$\theta_{in,A}$, $\theta_{out,A} \rightarrow \theta_{diff,A}$; $\theta_{out,B} = 0$	B_c	NS
ImpM	$\theta_{in,A}$, $\theta_{out,A} \rightarrow \theta_{diff,A}$	B_c	BPU/MP		ECM	$\theta_{in,A}$, $\theta_{out,A} \rightarrow \theta_{diff,A}$; $\theta_{out,B} = 0$	B_e	NS

Supporting Material

S1 ODE Model of encoder architectures:

We modeled all encoder architectures by simple sets of ODEs of the following form.

Architectures without SM modification:

$$\begin{aligned}\frac{d[A_c]}{dt} &= \Pi - \Theta_A - \Lambda_{Ac} \\ \frac{d[A_e]}{dt} &= \rho\Theta_A - \Lambda_{Ae}\end{aligned} \tag{S1}$$

Architectures with intracellular SM modification:

$$\begin{aligned}\frac{d[A_c]}{dt} &= \Pi - \Gamma - \Lambda_{Ac} \\ \frac{d[B_c]}{dt} &= \Gamma - \Theta_B - \Lambda_{Bc} \\ \frac{d[B_e]}{dt} &= \rho\Theta_B - \Lambda_{Be}\end{aligned} \tag{S2}$$

Architectures with SM modification during export:

$$\begin{aligned}\frac{d[A_c]}{dt} &= \Pi - \Theta_\Gamma - \Lambda_{Ac} \\ \frac{d[B_e]}{dt} &= \rho(\Theta_\Gamma - \Theta_B) - \Lambda_{Be} \\ \frac{d[B_c]}{dt} &= \Theta_B - \Lambda_{Bc}\end{aligned} \tag{S3}$$

Architectures with extracellular SM modification:

$$\begin{aligned}\frac{d[A_c]}{dt} &= \Pi - \Theta_A - \Lambda_{Ac} \\ \frac{d[A_e]}{dt} &= \rho\Theta_A - \Gamma - \Lambda_{Ae} \\ \frac{d[B_e]}{dt} &= \Gamma - \rho\Theta_B - \Lambda_{Be} \\ \frac{d[B_c]}{dt} &= \Theta_B - \Lambda_{Bc}\end{aligned} \tag{S4}$$

Architectures with SM modification during import:

$$\begin{aligned}
\frac{d[A_c]}{dt} &= \Pi - \Theta_A - \Lambda_{Ac} \\
\frac{d[A_e]}{dt} &= \rho(\Theta_A - \Theta_\Gamma) - \Lambda_{Ae} \\
\frac{d[B_c]}{dt} &= \Theta_\Gamma - \Theta_B - \Lambda_{Bc} \\
\frac{d[B_e]}{dt} &= \rho\Theta_B - \Lambda_{Be}
\end{aligned} \tag{S5}$$

Here Π is a constant production rate of molecules A_c, Θ_x is a transport term of molecules A, B or modifying transport for $x=A,B,\Gamma$ respectively, that is a linear function of the respective molecule concentration. Γ is the modification term, with $\Gamma = \gamma[A_y]$, where $y=c,e$ for intra- or extracellular modification, respectively. Λ_z is the degradation term of molecules z, with $\Lambda_z = \lambda_z [z]$. The cell density or volume fraction ρ takes into account the dilution during transport from the intracellular to extracellular volume.

S2 Steady State Concentration:

Using a constant production rate and assuming all other processes to be in the linear regime we can calculate the steady state concentration of the different encoder architectures.

No modification (NM; 6 architectures)

ODEs:

$$\begin{aligned}
\frac{d}{dt}[A_c] &= \pi - \theta_{out,A}[A_c] + \theta_{in,A}[A_e] - \lambda_{Ac}[A_c] \\
\frac{d}{dt}[A_e] &= \rho(\theta_{out,A}[A_c] - \theta_{in,A}[A_e]) - \lambda_{Ae}[A_e]
\end{aligned} \tag{S6}$$

Steady state:

$$\begin{aligned}
[A_c] &= \pi\left(\lambda_{Ac} + \frac{\theta_{out,A}\lambda_{Ae}}{\theta_{in,A}\rho + \lambda_{Ae}}\right)^{-1} \\
[A_e] &= \pi\theta_{outA}\rho\left(\lambda_{Ac}\theta_{in,A}\rho + \left(\lambda_{Ac} + \theta_{out,A}\right)\lambda_{Ae}\right)^{-1}
\end{aligned} \tag{S7}$$

With the steady state results we have the results for two different architectures with active import and export and get another four by setting $\Theta_{in;A} = 0$ (two architectures without re-import) or substituting $\Theta_{in;A}$ and $\Theta_{out;A}$ by $\Theta_{diff;A}$ (two architectures with diffusion). Thus we get three different 2-node structures resulting in 3x2 = 6 architectures.

Intracellular modification (ICM; 9 architectures)

ODEs:

$$\begin{aligned}\frac{d}{dt}[A_c] &= \pi - \gamma[A_c] - \lambda_{Ac}[A_c] \\ \frac{d}{dt}[B_c] &= \gamma[A_c] - \theta_{out,B}[B_c] + \theta_{in,B}[B_e] - \lambda_{Bc}[B_c] \\ \frac{d}{dt}[B_e] &= \rho(\theta_{out,B}[B_c] - \theta_{in,B}[B_e]) - \lambda_{Be}[B_e]\end{aligned} \tag{S8}$$

Steady state:

$$\begin{aligned}[A_c] &= \pi(\gamma + \lambda_{Ac})^{-1} \\ [B_c] &= \pi\gamma\left(\left(\lambda_{Bc} + \frac{\theta_{out,B}\lambda_{Be}}{\theta_{in,B}\rho + \lambda_{Be}}\right)(\gamma + \lambda_{Ac})\right)^{-1} \\ [B_e] &= \pi\gamma\theta_{out,B}\rho\left(\left(\lambda_{Bc}\theta_{in,B}\rho + (\lambda_{Bc} + \theta_{out,B})\lambda_{Be}\right)(\gamma + \lambda_{Ac})\right)^{-1}\end{aligned} \tag{S9}$$

With the steady state results we have the results for three different architectures with active import and export and get another six by setting $\theta_{in} = 0$ (three architectures without re-import) or substituting θ_{in} and θ_{out} by θ_{diff} (three architectures with diffusion). Thus we get three different 3-node structures resulting in 3x3 = 9 architectures.

Modification during export (ExpM; 11 architectures)

ODEs:

$$\begin{aligned}\frac{d}{dt}[A_c] &= \pi - \theta_\gamma[A_c] - \lambda_{Ac}[A_c] \\ \frac{d}{dt}[B_e] &= \rho(\theta_\gamma[A_c] + \theta_{out,B}[B_c] - \theta_{in,B}[B_e]) - \lambda_{Be}[B_e] \\ \frac{d}{dt}[B_c] &= \theta_{in,B}[B_e] - \theta_{out,B}[B_c] - \lambda_{Bc}[B_c]\end{aligned} \tag{S10}$$

Steady state:

$$[A_c] = \pi\left(\theta_\gamma + \lambda_{Ac}\right)^{-1}$$
$$[B_e] = \pi\theta_\gamma\rho\left(\left(\lambda_{Be} + \frac{\theta_{in,B}\lambda_{Bc}\rho}{\theta_{out,B} + \lambda_{Bc}}\right)\left(\theta_\gamma + \lambda_{Ac}\right)\right)^{-1} \quad \text{(S11)}$$
$$[B_c] = \pi\theta_\gamma\theta_{in,B}\rho\left(\left(\lambda_{Bc}\theta_{in,B}\rho + \left(\lambda_{Bc} + \theta_{out,B}\right)\lambda_{Be}\right)\left(\theta_\gamma + \lambda_{Ac}\right)\right)^{-1}$$

With the steady state results we have the results for three different architectures with active import and export and get another six by setting $\theta_{out} = 0$ (three architectures without re-export) or substituting θ_{in} and θ_{out} by θ_{diff} (three architectures with diffusion). Furthermore we get a 2-node structure by setting $\theta_{in} = 0$. Thus we get one 2-node and three 3-node structures resulting in 1x2 + 3x3 = 11 architectures.

Modification during Import (ImpM; 45 architectures)

ODEs:

$$\frac{d}{dt}[A_c] = \pi - \theta_{out,A}[A_c] + \theta_{in,A}[A_e] - \lambda_{Ac}[A_c]$$
$$\frac{d}{dt}[A_e] = \rho(\theta_{out,A}[A_c] - \theta_{in,A}[A_e] - \theta_\gamma[A_e]) - \lambda_{Ae}[A_e]$$
$$\frac{d}{dt}[B_c] = \theta_\gamma[A_e] + \theta_{in,B}[B_e] - \theta_{out,B}[B_c] - \lambda_{Bc}[B_c] \quad \text{(S12)}$$
$$\frac{d}{dt}[B_e] = \rho(\theta_{out,B}[B_c] - \theta_{in,B}[B_e]) - \lambda_{Be}[B_e]$$

Steady state:

$$[A_c] = \pi\left(\lambda_{Ac} + \frac{\theta_{out,A}(\lambda_{Ae} + \theta_\gamma\rho)}{(\theta_{in,A} + \theta_\gamma)\rho + \lambda_{Ae}}\right)^{-1}$$
$$[A_e] = \pi\theta_{outA}\rho\left((\lambda_{Ac}(\theta_{in,A} + \theta_\gamma) + \theta_{out,A}\theta_\gamma)\rho + \left(\lambda_{Ac} + \theta_{out,A}\right)\lambda_{Ae}\right)^{-1}$$
$$[B_c] = [A_e]\theta_\gamma\left(\theta_{out,B} + \lambda_{Bc} - \frac{\theta_{out,B}\theta_{in,B}\rho}{\theta_{in,B}\rho + \lambda_{Be}}\right)^{-1} =: [A_e][B_c]_2 \quad \text{(S13)}$$
$$[B_e] = [A_e]\theta_\gamma\theta_{out,B}\rho\left(\left(\lambda_{Bc} + \theta_{out,B}\right)\left(\theta_{in,B}\rho + \lambda_{Be}\right) - \theta_{out,B}\theta_{in,B}\rho\right)^{-1} =: [A_e][B_e]_2$$

With the steady state results we have the results for four different architectures with active import and export. By setting $\theta_{in,A} = 0$ (no re-import of molecules A) or substituting $\theta_{in,A}$ and $\theta_{out,A}$ by $\theta_{diff,A}$ (diffusion of molecules A) and $\theta_{in,B} = 0$ (no re-import of molecules B) or substituting $\theta_{in,B}$ and $\theta_{out,B}$ by $\theta_{diff,B}$ (diffusion of molecules B), we have three different transport mechanisms for each molecule leading

to nine possible combinations of 4-node structures. Furthermore we get three 3-node structures by setting $\theta_{out,B} = 0$. Thus we get three 3-node and nine 4-node structures resulting in 3x3 + 9x4 = 45 architectures.

Extracellular modification (ECM; 45 architectures)

ODEs:

$$\begin{aligned}
\frac{d}{dt}[A_c] &= \pi - \theta_{out,A}[A_c] + \theta_{in,A}[A_e] - \lambda_{Ac}[A_c] \\
\frac{d}{dt}[A_e] &= \rho(\theta_{out,A}[A_c] - \theta_{in,A}[A_e]) - \gamma[A_e] - \lambda_{Ae}[A_e] \\
\frac{d}{dt}[B_e] &= \gamma[A_e] + \rho(\theta_{out,B}[B_c] - \theta_{in,B}[B_e]) - \lambda_{Be}[B_e] \\
\frac{d}{dt}[B_c] &= \theta_{in,B}[B_e] - \theta_{out,B}[B_c] - \lambda_{Bc}[B_c]
\end{aligned} \tag{S14}$$

Steady state:

$$\begin{aligned}
[A_c] &= \pi\left(\lambda_{Ac} + \frac{\theta_{out,A}(\lambda_{Ae}+\gamma)}{\theta_{in,A}\rho + \gamma + \lambda_{Ae}}\right)^{-1} \\
[A_e] &= \pi\theta_{outA}\rho\left(\lambda_{Ac}\theta_{in,A}\rho + \left(\lambda_{Ac} + \theta_{out,A}\right)(\lambda_{Ae}+\gamma)\right)^{-1} \\
[B_e] &= [A_e]\gamma\left(\lambda_{Be} - \frac{\theta_{in,B}\lambda_{Bc}\rho}{\theta_{out,B} + \lambda_{Bc}}\right)^{-1} =: [A_e][B_e]_2 \\
[B_c] &= [A_e]\gamma\theta_{in,B}\left(\lambda_{Be}\left(\lambda_{Bc} + \theta_{out,B}\right) + \theta_{in,B}\lambda_{Bc}\rho\right)^{-1} =: [A_e][B_c]_2
\end{aligned} \tag{S15}$$

With the steady state results we have the results for four different architectures with active import and export. By setting $\theta_{in,A} = 0$ (no re-import of molecules A) or substituting $\theta_{in,A}$ and $\theta_{out,A}$ by $\theta_{diff,A}$ (diffusion of molecules A) and $\theta_{out,B} = 0$ (no re-export of molecules B) or substituting $\theta_{in,B}$ and $\theta_{out,B}$ by $\theta_{diff,B}$ (diffusion of molecules B), we have three different transport mechanisms for each molecule leading to nine possible combinations of 4-node structures. Furthermore we get three 3-node structures by setting $\theta_{in,B} = 0$. Thus we get three 3-node and nine 4-node structures resulting in 3x3 + 9x4 = 45 architectures.

S3 Analytical approximation of EM noise

We estimate the noise analytically from a heuristic noise model inspired by Ref.(37) by considering the relative noise being composed out of extrinsic and intrinsic contributions as follows:

$$\eta^2 = \frac{\sigma_{\text{int}}^2 + \sigma_{ext}^2}{\left(\langle n \rangle\right)^2}. \tag{S16}$$

Let $\langle . \rangle$ denote the average over intrinsic fluctuations and take the parameter set $\boldsymbol{P}$ as extrinsic variables. Then

$$\sigma_{\text{int}}^2 = \int d\boldsymbol{P}\, p(\boldsymbol{P})\left(\left\langle n(\boldsymbol{P})^2 \right\rangle - \left\langle n(\boldsymbol{P}) \right\rangle^2\right) = \int d\boldsymbol{P}\, p(\boldsymbol{P})\hat{\sigma}_{\text{int}}^2(\boldsymbol{P}), \tag{S17}$$

is the parameter averaged intrinsic noise, with $\hat{\sigma}_{\text{int}}^2(\boldsymbol{P})$ being the intrinsic noise for a given parameter set $\boldsymbol{P}$. The extrinsic noise is given by

$$\sigma_{ext}^2 = \int d\boldsymbol{P}\, p(\boldsymbol{P})\langle n \rangle^2 - \left(\int d\boldsymbol{P}\, p(\boldsymbol{P})\langle n \rangle\right)^2. \tag{S18}$$

By using the approximation $\int d\boldsymbol{x}\, p(\boldsymbol{x}) f(\boldsymbol{x}) \approx f(\boldsymbol{\mu}) + \frac{1}{2}\sum_i \sigma_{\text{i}}^2 \left.\frac{\partial^2 f(\boldsymbol{x})}{\partial x_i^2}\right|_{x=\mu}$ from Ref. (6) we get

$$\sigma_{\text{int}}^2 = \hat{\sigma}_{\text{int}}^2(\boldsymbol{\mu}) + \frac{1}{2}\sum_{i=1}^{N} \sigma_i^2 \left.\frac{\partial^2 \hat{\sigma}_{\text{int}}^2(\boldsymbol{P})}{\partial P_i^2}\right|_{\boldsymbol{P}=\boldsymbol{\mu}} \quad \text{and} \quad \sigma_{ext}^2 \approx \sum_{i=1}^{N} \sigma_{\text{i}}^2 \left(\left.\frac{\partial \langle n(\boldsymbol{P}) \rangle}{\partial P_i}\right|_{P=\mu} \right)^2. \tag{S19}$$

In order to calculate the total noise from these expressions the intrinsic noise $\hat{\sigma}_{\text{int}}^2$ has to be specified. Although linear biochemical processes do not in general generate Poissonian noise, a variance scaling linear with the mean is still often a good approximation at least to first order (7). Therefore we assume that the intrinsic noise for a given set of parameters $\boldsymbol{P}$ is proportional to the mean particle number, i.e. $\hat{\sigma}_{\text{int}}^2(\boldsymbol{P}) = a \cdot \langle n(\boldsymbol{P}) \rangle$, we get for the relative noise:

$$\eta^2 = \frac{1}{\langle n(\boldsymbol{\mu}) \rangle^2}\left(a \cdot \langle n(\boldsymbol{\mu}) \rangle + \frac{1}{2} a \sum_{i=1}^{N} \sigma_{\text{i}}^2 \left.\frac{\partial^2 \langle n(\boldsymbol{P}) \rangle}{\partial P_i^2}\right|_{P=\mu} + \sum_{i=1}^{N} \sigma_{\text{i}}^2 \left(\left.\frac{\partial \langle n(\boldsymbol{P}) \rangle}{\partial P_i}\right|_{P=\mu} \right)^2 \right). \tag{S20}$$

We find this result to match the numerical simulations very well for a=1 and find the result

$$\eta^2 = \frac{1}{\langle n(\boldsymbol{\mu}) \rangle^2}\left(\langle n(\boldsymbol{\mu}) \rangle + \frac{1}{2} \sum_{i=1}^{N} \sigma_{\text{i}}^2 \left.\frac{\partial^2 \langle n(\boldsymbol{P}) \rangle}{\partial P_i^2}\right|_{P=\mu} + \sum_{i=1}^{N} \sigma_{\text{i}}^2 \left(\left.\frac{\partial \langle n(\boldsymbol{P}) \rangle}{\partial P_i}\right|_{P=\mu} \right)^2 \right), \tag{S21}$$

which is Eq.4 in the main text. The mean particle number in steady state is obtained from the steady state concentration from the ODE-model by multiplying with V_c or V_p, respectively.

S4 Parameters

The example systems used for generating the plots in the main text are highlighted in supporting table S3.

We used a standard set of parameter values which fall into the physiological range or reported values from natural systems (5): The production rate was taken as $\pi = 10000$ nM/h, all transport rates as well as modification rates were taken as $\theta_x = \gamma = 300\ h^{-1}$ (x = A,diff, B,diff, A,in, B,in, A,out, B,out, γ) and all degradation rates were taken as $\lambda_z = 0.1\ h^{-1}$ ($z = A_c, B_c, A_e, B_e$). These parameters were used throughout all plots and calculations for all nonzero parameter values, with the following exceptions:
For the band-pass ultrasensitive and multi-pass architectures shown in figure 4, which are the only systems where the qualitative encoding scheme changes with parameters, we kept all parameters as in our generic set and changed θ_γ to 3 h^{-1} and 3000 h^{-1} and λ_{A_e} to 10 h^{-1} and 0.01 h^{-1} for band-pass ultrasensitive and multi-pass behavior, respectively. Furthermore we used for the low-pass ultrasensitive system in Fig.4 the same set of parameters as for the multi-pass and for the negative sensitivity a modification rate $\gamma = 100\ h^{-1}$, for the sake of a better visibility of the relevant effects.

For the stochastic simulations, additional parameters are required, namely the parameter noise σ_i, the cell volume V_c the cell proximate volume V_p and the exchange rate between V_p and the environment. We took $V_p = V_c = 10^{-15}$l and particle exchange rates between V_p and the environment that are 4 orders of magnitude larger than the fasted transport rate. We furthermore assume that the parameter noise σ_i is 10% of the respective mean μ_i.

S5 Definition of four basic classes of encoder architectures

Though [*SM*], ε and η^2 of each signaling architecture depend strongly on the respective model parameters, all 2-and 3-node networks as well as all 4-node networks sensing the unmodified molecules A can be ordered in one of four classes (Fig. 2 in the main text).

Non-functional class (NF)

NF architectures are insensitive to changes in the input ρ, i.e. $\varepsilon = 0$ or $[SM](\rho) = \text{const}$. As the SM concentration is independent of the input ρ, also the noise of these networks is independent of the input, i.e. $\eta(\rho) = \text{const}$. All architectures in the non-functional class sense the intracellular SM concentration (A_c or B_c) that is produced intracellular and exported but not re-imported. Therefore this concentration does not contain any information about the environment and is insensitive to changes in the input ρ.

Band-pass class (BP)

For BP architectures the SM concentration and signal sensitivity can be written in the form

$[SM](\rho) = (\rho + a)/(b\rho + k)$

and

$$\varepsilon(\rho) = (k - ab)\rho /((a + \rho)(k + b\rho)), \quad \text{(S22)}$$

where a, b and k depend on the model parameters (such as production rate, transport rate, degradation rate, etc.) of the respective architecture and may be very different among different architectures. In BP architectures the noise remains relatively small over the whole input range ($0 \leq \rho \leq \infty$), with the extrinsic noise η_{ext} being the dominant contribution. This is due to the fact, that even at small cell densities the SM concentration does not drop below some basal level, thereby keeping the intrinsic fluctuations small, as they result from small molecule numbers. Members of the band-pass class re-import the extracellular SMs. Due to the re-import the extracellular SM concentration saturates at high cell densities because of the increasing number of consumers. Therefore also the intracellular SM concentration does not increase above some saturation level at high cell densities, but it also does not fall below some basal level at low cell densities. This is due to the fact, that these architectures sense the intracellular SM concentration of SMs that are produced intracellular. This leads to a basal intracellular SM level even in a single cell in a huge extracellular volume. Therefore $\varepsilon \rightarrow 0$ for high and low cell densities, with $0 < \varepsilon < 1$ at an intermediate regime. For $\rho_{max} = (ak)^{1/2} b^{-1/2}$ the sensitivity reaches its maximal value $\varepsilon_{max} = \varepsilon (\rho_{max}) = (k^{1/2} - a^{1/2} b^{1/2})(k^{1/2} + a^{1/2} b^{1/2})^{-1}$ that depends on the parameter values of the system.

Low-pass class (LP)

For LP architectures the SM concentration and signal sensitivity can be written in the form

$$[SM](\rho) = \rho/(b\rho + k) \quad \text{(S23)}$$

and

$$\varepsilon(\rho)= k/(k+ b\rho), \quad \text{(S24)}$$

where b and k depend on the model parameters (such as production rate, transport rate, degradation rate, etc.) of the respective architecture and may be very different among different architectures. In LP architectures the noise diverges for $\rho \rightarrow 0$ and decreases with increasing ρ to some basal level, determined by the extrinsic noise η_{ext}. With decreasing ρ the SM concentration decreases with $[SM](\rho) \rightarrow 0$ as $\rho \rightarrow 0$ therefore the intrinsic noise diverges as $\rho \rightarrow 0$. With increasing ρ the SM concentration increases and thus the noise at large ρ is mainly determined by the noise induced by parameter fluctuations η_{ext}. However, in LP architectures the noise may take on some minimal value at intermediate ρ-values. Members of the low-pass class re-import the extracellular SMs either unmodified or with modification during import and sense either the extracellular SM concentration or the modified intracellular concentration. Due to the re-

import the SM concentration saturates at high cell densities because of the increasing number of consumers. Therefore their sensitivity drops to zero at high cell densities while it approaches 1 for small cell densities.

Ideal class (ID)

While ε depends on the input ρ in classes BP and LP, the signal sensitivity is constant for class ID. We found for ID architectures $\varepsilon = 1$, i.e. the steady state SM concentration is proportional to ρ ($[SM](\rho) \propto \rho$). The noise in ID architectures behaves in the same qualitative way as in LP architectures, for the same reasons. However, it does not exhibit a minimal value but decreases monotonically with increasing ρ. All architectures, that are members of the ideal class, sense the extracellular concentration and do not re-import the SMs that are sensed. This means all these architectures export the SMs at a constant steady state rate and do not consume the SMs once they are exported. Therefore the SM concentration is always proportional to the cell density (i.e. for a fixed extracellular volume the number of SM producing cells) and does not saturate at high or low cell densities.

S6 Decomposition of 4-node networks

In the more complex 4-node networks the initially produced SMs A_c are exported without modification and are afterwards modified during import or in the extracellular volume. We found that these networks can be either reduced to one 2-node network or decomposed into two 2-node networks, depending on whether the unmodified (A) or modified (B) SMs are sensed by the signaling architecture. Signaling architectures that sense the unmodified SMs A are independent of all processes that follow the modification step, while the signal modification only plays the role of an additional contribution to degradation. Therefore these systems can be truncated at the modification step and thereby reduced to effective 2-node networks. All arguments used for the 2-node networks apply also for these networks and the classification depends only on the properties of the truncated network. 4-node networks that sense the modified SMs (B) on the contrary cannot be reduced to a single 2-node network as the processes of the ”unmodified” sub-network still influences the behavior of the whole network. However, it is possible to separate the “unmodified” from the “modified” sub-network thereby decomposing the 4-node network into two effective 2-node networks. Again the arguments of classification hold true for the two sub-networks, while the sensitivity ε of the complete 4-node network is the sum of the sensitivities of the sub-networks. To make these statements more precise we can denote the output signals of each sub-network as $[A_x]_2$ and $[B_x]_2$ (x = c, e) for the unmodified and the modified sub-network respectively and for the full 4-node networks $[A_x]_4$ and $[B_x]_4$ (x = c, e). With these notations we find

$$[A_x]_4(\rho)=[A_x]_2(\rho)$$

(S25)

$$[B_x]_4(\rho)=[A_e]_2(\rho) \times [B_x]_2(\rho). \quad \text{(S26)}$$

Applying the definition of ε (Eq. (2) in the main text) to Eq. (S26) yields for the modified 4-node networks

$$\varepsilon_{B4}(\rho) = \frac{\partial \log([B_x]_4)}{\partial \log \rho} = \frac{\partial \log([A_e]_2 \times [B_x]_2)}{\partial \log \rho} = \frac{\partial \log([A_e]_2)}{\partial \log \rho} + \frac{\partial \log([B_x]_2)}{\partial \log \rho} = \varepsilon_{A2}(\rho) + \varepsilon_{B2}(\rho) \quad \text{(S27)}$$

Thus the 4-node networks sensing the modified SMs are compositions of two simpler 2-node sub-networks with the sensitivity of the whole network being the sum of the sensitivities of the sub-networks. While the first of these 2-node sub-networks has the same structure in all 4-node networks, the second can be of two different types depending on whether the SM modification takes place during import or in the extracellular volume. The former results in two 2-node networks of the same structure with the SMs produced intracellular and exported into the extracellular volume (Fig. 3 B in the main text). The latter results in two 2-node networks, with the second expressing an inverted structure (Fig. 3 C in the main text), i.e. the SMs being produced extracellular and then imported into the cell. This inverted network structure causes some unexpected effects. The general behavior of the inverted network is the same as in the regular 2-node networks, with the only difference that the extracellular and the cellular volume V_e and V_c change roles. As we consider the cell density, i.e. the volume fraction of cells, $\rho = V_c/V_e$ as the input of the system, the input is thus inverted in the inverted network ($\rho \rightarrow 1/\rho$). This implies that $\varepsilon \rightarrow -\varepsilon$ as can be easily seen by the following consideration. Let $[SM](\rho)$ denote the SM concentration of a regular network and $[SM]^*(\rho)$ of the inverted network of the same structure. Than one obtains $[SM](\rho)=[SM]^*(1/\rho)$ and therefore

$$\varepsilon_{[SM]^*}(\rho) = \frac{\partial \log([SM]^*(\rho))}{\partial \log \rho} = \frac{\partial \log([SM](1/\rho))}{\partial \log \rho} = \frac{\partial \log([SM](1/\rho))}{\partial \log(1/\rho)} = -\varepsilon_{[SM]}(1/\rho) \quad \text{(S28)}$$

Thus the sensitivity of the inverted network ranges from -1 to 0, meaning that the SM concentration decreases with increasing cell density. From Eq.(S1) follows that 4-node networks with SM modification during import can express a sensitivity larger than one, namely $2 \geq \varepsilon \geq 0$, i.e. the SM concentration depends stronger than linear on ρ (Fig. 3 A in the main text). However 4-node networks with SM modification in the extracellular volume can express a positive as well as a negative sensitivity, namely $1 \geq \varepsilon \geq -1$, i.e. the SM concentration can increase as well as decrease with increasing ρ (Fig. 3 A in the main text). There is a variety of combinations of classes depending on the details of the two sub-networks. In Figure 3 in the main text are examples of LP + BP, LP + LP, LP + ID, LP + NF, LP + INV and ID + INV. These are all possible combinations as in networks with modification during import the first sub-network is always a LP, because import is always present, due to the modification step, therefore

excluding ID networks and the extracellular SM concentration is relevant therefore excluding classes BP and NF. In networks with extracellular modification, the first sub-network can be either LP or ID while the second is always an inverted network as the SMs are produced extracellular.

Next we analyzed the noise characteristics of the 4-node networks composed of two 2-node sub-networks, described above. The total noise in these network architectures can be decomposed into the noise of the sub-networks as we did with the signal sensitivity. However η^2 is not simply the sum of the noise of the subsystems as it is the case for ε. The decomposition has rather to be done for the extrinsic and intrinsic part of the noise individually. As we pointed out above the SM concentration can be written as the product of the SM concentrations of the sub-networks (Eq. (S1)), thus also the intrinsic noise η^2 can be approximated by the product of the intrinsic noise of the sub-networks as it depends at zeros order on the SM number. On the contrary the extrinsic noise is the sum of the contributions of parameter fluctuations, thus the extrinsic noise η^2 can be approximated by the sum of the extrinsic of the sub-networks. Unlike the decomposition of the sensitivity ε, that gives the exact result, the noise decomposition only approximates the true result. However, the general qualitative behavior can still be found from the decomposition into two 2-node networks (Supporting Fig. S2). While the noise in the simple 2-and 3-node networks only diverges for $\rho \to 0$, 4-node networks composed of a regular and an inverted 2-node network can express divergent noise also for $\rho \to \infty$. This is due to the fact that these networks express the counterintuitive feature of decreasing SM concentrations for increasing cell densities ρ.

Supporting References

1. Bassler, B.L., E.P. Greenberg, and a M. Stevens. 1997. Cross-species induction of luminescence in the quorum-sensing bacterium Vibrio harveyi. J Bacteriol. 179: 4043–5.

2. Macinga, D.R., M.M. Parojcic, and P.N. Rather. 1995. Identification and analysis of aarP , a transcriptional activator of the 2 ’ -N-acetyltransferase in Providencia stuartii . J. Bacteriol. 177: 3407–13.

3. Lassak, J., A.-L. Henche, L. Binnenkade, and K.M. Thormann. 2010. ArcS, the cognate sensor kinase in an atypical Arc system of *Shewanella oneidensis* MR-1. Appl. Environ. Microbiol. 76: 3263–74.

4. Fried, L., J. Lassak, and K. Jung. 2012. A comprehensive toolbox for the rapid construction of lacZ fusion reporters. J. Microbiol. Methods. 91: 537–43.

5. Pai, A., and L. You. 2009. Optimal tuning of bacterial sensing potential. Mol Syst Biol. 5: 1–11.

6. Swain, P.S., M.B. Elowitz, and E.D. Siggia. 2002. Intrinsic and extrinsic contributions to stochasticity in gene expression. Proc Natl Acad Sci U S A. 99: 12795–800.

7. Van Kampen, N.G. 2007. Stochastic Processes in Physics and Chemistry. 3rd ed. Amsterdam: Elsevier B.V.